Asteroid Impact Risk: Ground Hazard versus Impactor Size

Donovan Mathias[1], Lorien Wheeler[2], Jessie Dotson[1], Michael Aftosmis[1], and Ana Tarano[3]
[1]NASA Ames Research Center, [2]CSRA/NASA Ames Research Center, [3]STC/NASA Ames Research Center/Stanford University

Overview

We utilized a probabilistic asteroid impact risk (PAIR) model to stochastically assess the impact risk due to an ensemble population of Near-Earth Objects (NEOs). Concretely, we present the variation of risk with impactor size. Results suggest that large impactors dominate the average risk, even when only considering the subset of undiscovered NEOs.

Modeling Approach

The probabilistic asteroid impact risk model [1] uses Monte Carlo sampling to produce stochastic sets of potential impact scenarios based on uncertainty distributions characterizing key asteroid parameters. For each impact case, the entry and fragmentation process is modeled to compute the energy deposited in the atmosphere, determine airburst altitude or surface impact, and estimate the resulting damage areas and affected populations. Local damage due to blast overpressure and thermal radiation is assessed for land impacts, while regional damage due to asteroid-generated tsunami is assessed for impacts over the oceans. Local and regional damage include the latitude and longitude of the impact location and the globally distributed human population [11]. Global effects are considered for impact energies greater than 40 Gt and are independent of specific impact location. The impact consequences are combined with corresponding impact frequencies [2] to produce an estimate of the ensemble impact risk.

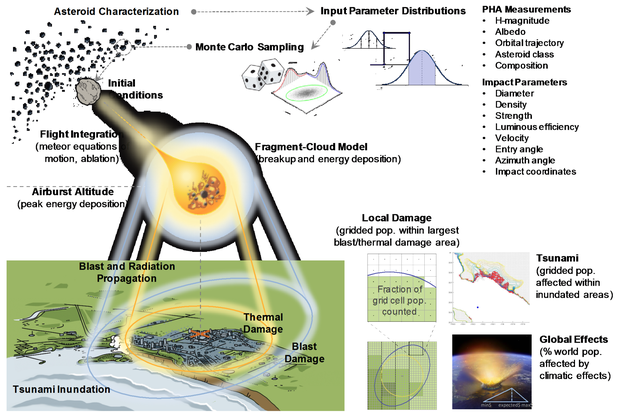

An innovative fragment-cloud model (FCM) [3,4] is used to generate energy deposition curves as the asteroid enters the Earth's atmosphere. FCM integrates the entry trajectory, accounting for aerodynamic heating and drag, until the stagnation pressure exceeds the "aerodynamic strength" of the object, at which point fragmentation begins. Each fragmentation event breaks the parent object into a set of discrete fragments and a debris cloud. The fragments gain strength according to their reduced size and continue descent until their new strength is exceeded and they break again, or until they ablate completely or impact the surface. The cloud is assumed to have lost its strength and is allowed to rapidly disperse, depositing its energy in the process. An energy deposition curve is produced and used for the subsequent ground hazard assessment.

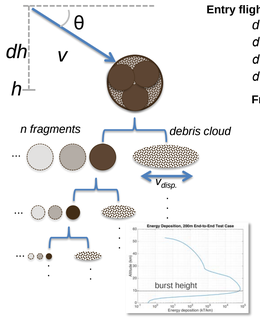

Entry flight: integrates meteor equations of motion and ablation

$$dm/dt = -0.5\rho_{air}v^3A\sigma$$
$$dv/dt = \rho_{air}v^2AC_D/m - gsin\theta$$
$$d\theta/dt = (v/(R_E+h) - g/v)cos\theta$$
$$dh/dt = vsin\theta$$

Fragmentation when pressure > strength

$$\rho_{air}v^2 > strength$$

Each break yields:
- Multiple independent, identical fragments (baseline 2)
- Debris cloud of specified mass fraction (baseline 50%)

Fragment strengths increase with decreased size

$$S_2 = S_1(m_1/m_2)^\alpha$$

Clouds broaden and slow under common bow shock

$$v_{dispersion} = v_{cloud}(3.5\rho_{air}A/\rho_{cloud})^{1/2}$$

Energy deposition computed as change in total KE of all fragments/clouds as a function of altitude.

Airburst at altitude of peak energy deposition.

The local damage models use the height of burst and kinetic energy to establish an equivalent energy source for blast waves and thermal radiation. Empirical damage radii [5] plots, derived from relative small energy events, are combined with computational models to establish a distance at which the resulting blast wave drops to a specified level of overpressure. Thermal radiation is modeled assuming all of the energy is distributed over a hemispherical surface, following Collins [6].The larger of the blast or thermal damage radii is used for the casualty estimation.

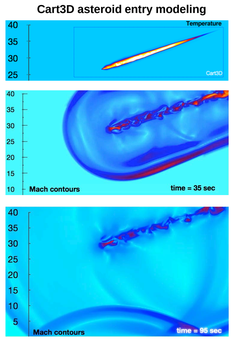

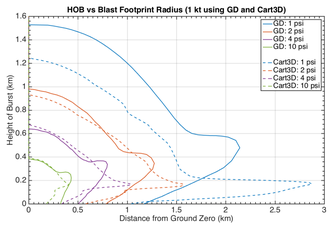

To the left is an example of blast wave propagation using Cart3D [10]. Above is a comparison of empirical and computational results at different yields normalized to 1 kt.

For water impacts, the kinetic energy remaining at the surface is scaled [7] and used to create an initial water impact crater [8]. The resulting wave is propagated to shore where it is assumed to shoal following the approach of Chesley and Ward [8]. Shoaled wave heights are compared to the local topography to produce flood maps, which are combined with fragility curves [9] to produce damage and casualty estimates. Global effects are assumed to scale with impact energy.

Quantifying Hazards

Hazard models determine the scope of ground damage for local, regional, and global hazards. The following illustrate how the hazard models are converted to casualties for each impact scenario [5] [6] [12].

Damage Level	Blast Threshold (psi)	Thermal Threshold Φ_1MT (MJ/m^2)	Population fraction
Serious	1 (window breakage and some structural damage)	0.25 (2nd degree burns)	0.1
Severe	2 (doors and windows blown out, widespread structural damage)	0.42 (3rd degree burns)	0.3
Critical	4 (most residential structures collapse)	0.84 (cotton/denim clothing ignites)	0.6
Unsurvivable	10 (complete devastation)	1.2 (sand explodes, roll roofing ignites)	1.0

Top: Hazard models are used to compute ground areas associated with overpressure and thermal radiation for four damage levels, shown above. The larger of blast/thermal is used for each damage level, and the affected population is computed. The population fraction in the right column is used to convert population within the damage regions to affected population or casualties.

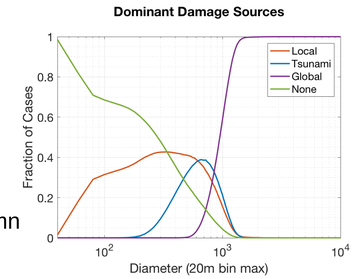

Bottom: Dominant damage source is shown as a function of object size. Below 300m, the most likely outcome is no casualties. Blast and thermal drive damage for the most cases between 300-600m. Tsunami is the largest fractional damage source for impactors 600-800m, and global effects dominate for objects >900m. Note that this plot shows the fraction of the simulated scenarios driven by each hazard, not the relative rate of casualties.

Risk Assessment

Risk differs from hazard in that risk includes the likelihood along with the consequence of an event. This section shows the quantitative risk results using the expected values as well as the output distributions.

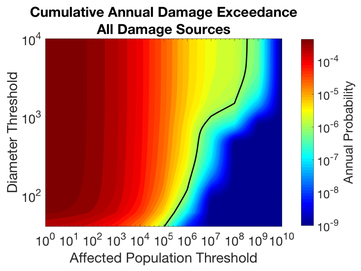

Contours represent the annual likelihood that a given population, or greater, will be affected by an object of a given size or smaller. The black line on the contour plots represents the 1-in-a-million per year probability. While the most severe consequences arise from large impacts, significant casualties are much more likely to arise from smaller impacts and blast/thermal damage.

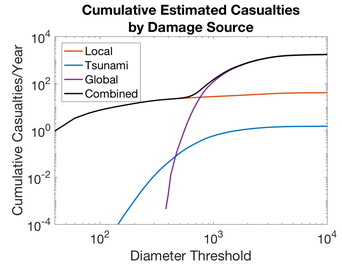

This plot shows the cumulative number of expected casualties per year, by damage source, as a function of impactor size. Two primary differences are seen compared to the previous plot. This figure includes the mean *consequence* and *likelihood* attributed to each impact scenario. Casualties are driven by local damage for impactors <500m and by global effects for larger objects. The relative consequence of tsunami is low compared to other sources.

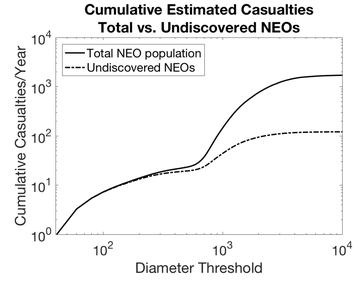

We now compare the cumulative annual expected casualties for the total NEO population to the fraction of currently undiscovered objects. The difference between curves represents the reduction in *perceived risk* due to object discovery. Below 300m, the curves remain within a factor of 2, but for objects 1km and larger differ by an order of magnitude. This represents the belief that most large NEOs have been detected and pose little near-term threat to the Earth.

Conclusions

Average casualties are dominated by large impacts causing global effects. However, when considering only the undiscovered fraction of NEOs, the average cumulative risk decreases by an order of magnitude. At smaller impactor sizes, the annual expected casualty estimates are dominated by blast and thermal damage.

Acknowledgements and References

This work was funded by the NASA Planetary Defense Coordination Office. REFERENCES: [1] D. Mathias, L. Wheeler, and J. Dotson, " A probabilistic asteroid impact risk model: assessment of sub-300 m impacts," Icarus 289 (2017), pp. 106-119, [2] A. Harris, "The population of near-Earth asteroids," *Icarus*, vol. 257, pp. 302–312, September 2015 , [3] P. Register, D. Mathias, and L. Wheeler, "Asteroid Fragmentation Approaches for Modeling Atmospheric Energy Deposition," Icarus 284C (2017) pp. 157-166, [4] L. Wheeler, D. Mathias, and P. Register, "A Fragment-Cloud Approach for Modeling Asteroid Breakup and Atmospheric Energy Deposition," Icarus 295 (2017), pp. 149-169, [5] S. Glasstone and P.J. Dolan, "The Effects of Nuclear Weapons," U.S. Government Printing Office, Washington D.C., 1977 , [6] G. Collins, H. J. Melosh, and R. Marcus, "Earth Impact Effects Program: A Web-based Computer Program for Calculating the Regional Environmental Consequences of a Meteoroid Impact on Earth," Meteoritics and Planetary Science, vol. 40, no. 6, pp. 817-840, 2005 , [7] L. Wheeler, D. Mathias, and P. Register, "Analytic Tsunami Models for Physics-Based Impact Risk Assessment", Second International Workshop on Asteroid Threat Assessment: Asteroid-generated Tsunami (AGT) and Associated Risk Assessment, Seattle, WA., August 2016, [8] S. Chesley and S. Ward, "A Quantitative Assessment of the Human and Economic Hazard from Impact-generated Tsunami," Natural Hazards (2006), [9] S. Koshimura, S. Hayashi, and H. Gokon, "Lessons from the 2011 Tohoku Earthquake Tsunami Disaster," Journal of Disaster Research, Vol.8, No.4, 2013, [10] M. Aftosmis, M. Berger and J. Melton, "Robust and Effcient Cartesian Mesh Generation for Component-Based Geometry," AIAA Journal, Vol. 36, No. 6, June 1998, pp. 952–960, [11] Center for International Earth Science Information Network - CIESIN - Columbia University, United Nations Food and Agriculture Programme - FAO, and Centro Internacional de Agricultura Tropical - CIAT. 2005. Gridded Population of the World, Version 3 (GPWv3): Population Count Grid. Palisades, NY: NASA Socioeconomic Data and Applications Center (SEDAC), [12] C. Rumpf, H. Lewis, and P. Atkinson, "Population Vulnerability Models for Asteroid Impact Risk Assessment," Meteoritics and Planetary Science 52(6), 2017, [13] G. Stokes et al., "Study to Determine the Feasibility of Extending the Search for Near-Earth Objects to Smaller Limiting Diameters," National Aeronautics and Space Administration, 2003.